



Research article

Synergistic effect of GO/ZnO loading on the performance of cellulose acetate/chitosan blended reverse osmosis membranes for NOM rejection

Rizwana Shami^{a,c,*}, Aneela Sabir^{a,**}, Sadia Sagar Iqbal^b, Nafisa Gull^{a,***}, Rubab Zohra^c, Shahzad Maqsood Khan^a

^a Institute of Polymer and Textile Engineering, University of the Punjab, Lahore, 54590, Pakistan

^b Department of Physics, Fatima Jinnah Women University, Rawalpindi, Pakistan

^c Department of Chemistry, Forman Christian College University, Lahore, Pakistan



ARTICLE INFO

Keywords:

Cellulose acetate
Chitosan
RO membranes
Graphene oxide
Zinc oxide

ABSTRACT

Declining freshwater resources along with their pollution are threatening the life existence on earth. To meet the freshwater demand, one of the most appropriate and possible ways which has been adopted all over the world is to reuse wastewater by removing its impurities. Among many water pollutants, natural organic matter (NOM) is found to be responsible as major precursor for the formation of other pollutants. Removal of NOM from wastewater is being done by using membrane filtration systems incorporated with certain nanofillers to increase membranes efficiency and permeability. In this study, novel nanocomposite reverse osmosis (RO) membranes were prepared using cellulose acetate and chitosan in *N,N*-Dimethyl formamide. Graphene oxide (GO) nanosheets and zinc oxide (ZnO) in different concentration were loaded to modify the membranes for tuning their RO performance. The confirmation of the functional groups is demonstrated by Fourier transform infrared spectroscopy which revealed the specific peaks indicating the formation of the nano-composite membranes. The surface morphology was studied by scanning electronic microscopy which shows a gradual transformation of the membrane surface from voids-free to macro-voids filled surface up to threshold concentration of GO and ZnO. The thermal properties of GO based membranes were analyzed using thermogravimetric analysis and differential scanning calorimetry. The uniform interaction of the GO and ZnO with polymers induced the remarkable thermal properties of the synthesized membranes. Permeate flux and contact angle measurements were considered to estimate their water content (96%) capacity and NOM rejection (96%) using 0.1 ppm humic acid solution. The permeate flux, NOM rejection and the water content changed directly with GO and inversely with ZnO wt% in the membranes up to GO5 (GO:0.14: ZnO:0.03) whereas the contact angle exhibited the inverse relationship with GO and ZnO concentration in casting solution of the synthesized membranes. Hence it can be concluded that prepared RO membranes are suitable for NOM rejection and recommended for water treatment.

* Corresponding author. Institute of Polymer and Textile Engineering, University of the Punjab, Lahore, 54590, Pakistan.

** Corresponding author.

*** Corresponding author.

E-mail addresses: rizshami99@gmail.com (R. Shami), aneela.ipte@pu.edu.pk (A. Sabir), nafisagull.ipte@pu.edu.pk (N. Gull).

<https://doi.org/10.1016/j.heliyon.2023.e13736>

Received 26 November 2022; Received in revised form 9 February 2023; Accepted 9 February 2023

Available online 15 February 2023

2405-8440/© 2023 The Authors. Published by Elsevier Ltd. This is an open access article under the CC BY-NC-ND license (<http://creativecommons.org/licenses/by-nc-nd/4.0/>).

1. Introduction

Water is the most essential ingredient for the existence of life for all living beings on earth. It's really alarming that only 0.8% of total water resources is available as potable water because 97% water is owned by oceans and 2% is enslaved by polar ice-caps and glaciers [1]. This distribution of water resources has raised a tough situation for limited potable water assets all over the world. Apart from limited supplies of potable water, other human accomplishments have been adversely affected due to scarcity of water such as agriculture, livestock production, industrialization, urbanization and many more [2]. It is very difficult to increase the supply of potable water due to immense increase in global population, urbanization, industrialization and climatic challenges [3]. All of these factors, in turn, have increased the immense pressure on the resources of fresh water. However, fresh and potable water resources can be saved and used wisely by reusing the wastewater for the activities such as agriculture, industry and urbanization [4,5].

To reuse the wastewater, techniques are required which must be energy efficient, less time consuming as well as cost-effective [6, 7]. Dilution of wastewater could be an effective method to decrease the micro pollutants in wastewater but these micro pollutants can pass through conventional water treatment method due to their nano size. Other than this, using activated sludge and biological filtering techniques also pay no serious service to the desired level as most of pollutants remain soluble in effluents [8–10]. Certain other physicochemical treatments such as coagulation and flocculation also proved to be inefficient to remove dissolved organic compounds in numerous studies [11–13]. Another possible method in this regard is chlorination which positively inhibits the regrowth of bacteria and pathogens [14] but has more adverse effects on reclaimed water. It not only decreases the organoleptic characteristics of reclaimed water but also generates disinfection by-products [15] while reacting with the dissolved natural organic matter (NOM) in wastewater. NOM consists of carboxylic acids, humic substances, amino acids, proteins, polysaccharides and hydrocarbons [16–18]. The physicochemical properties of NOM differ according to source and age of wastewater as well as season. Hence removal of NOM has become a pronounced challenge for water services and cost and energy efficient technologies are the dire need for the treatment of wastewater [19].

Membrane filtration technology has been found very effective among other technologies because of its extraordinary performance, low cost and comfort of operation [20]. This technology has potential applications in various fields including desalination, bio-purification, gas and liquid phase pollutant capture, gas separation, heavy metals removal, dyes removal, removal of NOM from wastewater etc. Numerous materials and methodologies have gained attention to develop the membranes with high flux rate along with high rejection of the desired impurities since last many decades [21]. An extensively and frequently accepted material for the synthesis of a hydrophilic membrane is cellulose acetate (CA) [22]. It is one of the most candid polymers due to its easy availability, low price, reasonable chlorine resistance, worthy biocompatibility and high hydrophilicity [23]. However, the hydrophilic nature of CA affects the diffusion of water and retards coagulation during its synthesis by phase inversion method and thus produces a dense skin layer with low permeate flux [24]. Therefore, modification of CA membrane is required while blending it with some other exceptional performance polymers [25] as well as with nano-particles. Chitosan (CS) has been added to CA as it has been found an excellent membrane supporting material because of its high film forming capability, biocompatible nature and ease of modification. To improve the qualities of CA membranes, one of the recently revealed nano-material is graphene oxide (GO) due to its convenient availability, chemical stability and extraordinary mechanical strength [26] as it can increase the membrane performance regarding its flux rate and rejection [27,28]. Recent advancement in nanomaterials has also exposed other hydrophilic materials for example silica, alumina, zinc oxide (ZnO) and zeolite. Among all these, ZnO is most suitable due to its antibacterial properties and chemical stability [29,30]. Conversely, up to best of our knowledge regarding RO membranes being used for the removal of NOM, no research has been done to study the effect of GO/ZnO content incorporated in the blend of CA and CS. Hence, the objectives behind this study are successful fabrication of GO/ZnO based polymer composite membranes and investigation of performance of these membranes varying in concentration of GO/ZnO regarding permeate flux and NOM rejection.

In this study, GO and ZnO have been merged in mixed matrix ultrafiltration (UF) and nanofiltration (NF) membranes. Such nano-hybrid filtration membranes have shown a significant performance regarding high water flux, contamination rejection, antifouling and antibacterial phenomenon.

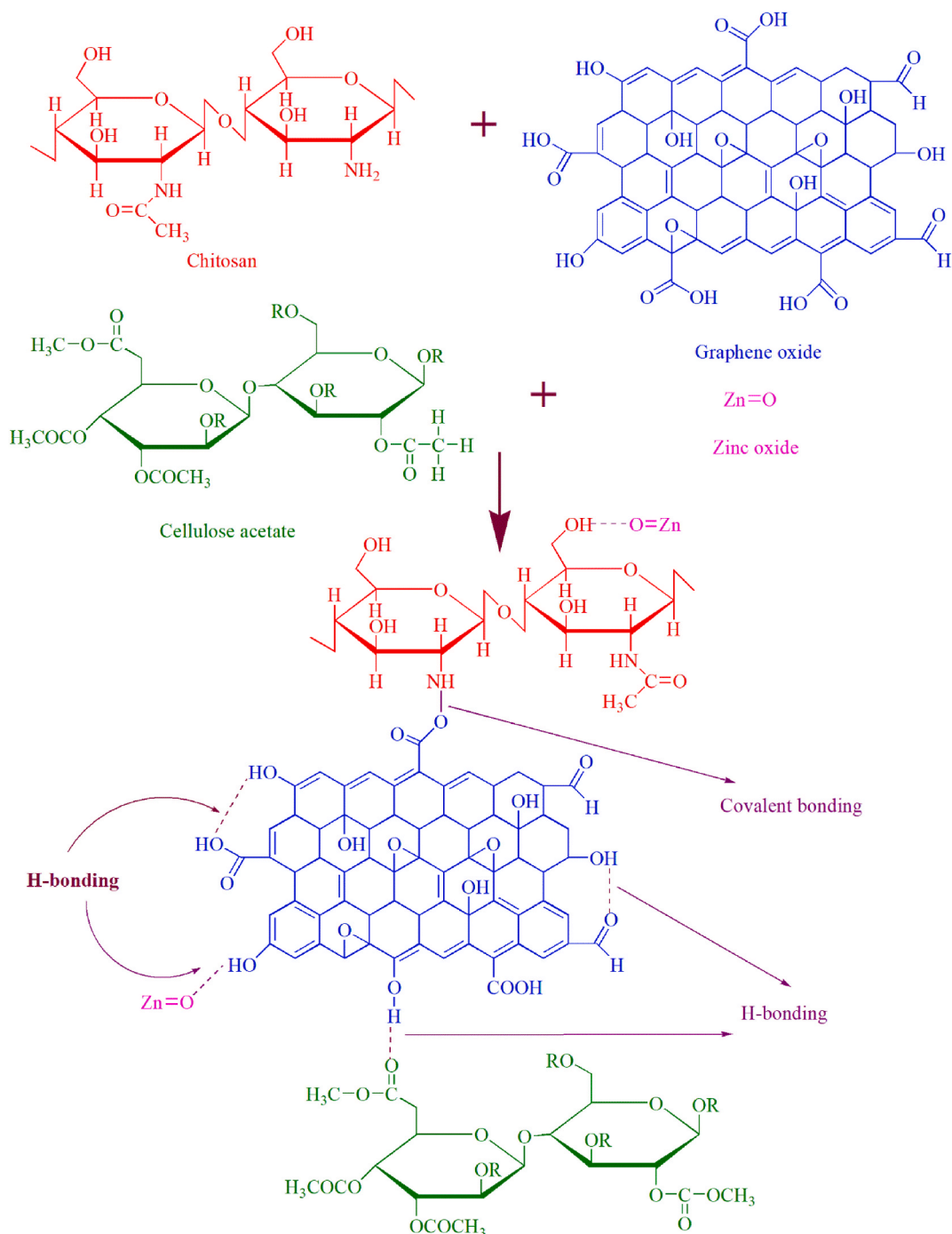
2. Experimental design

2.1. Materials

Cellulose acetate (CA) with 39.7% acetyl content of analytical grade was purchased from Fluka (USA), chitosan (CS) (Mol. Wt 1800,000 g/mol) was bought from Sigma Aldrich, graphene oxide (GO) and zinc oxide (ZnO) with 99.7% purity were obtained from Inframat Advance Materials (USA). *N,N*-dimethyl formamide (DMF) got from Fluka, USA were used for the preparation of membranes whereas humic acid (HA) from Sigma Aldrich was used to test the RO performance of synthesized membranes. No further purification was carried out for these chemicals.

2.2. Synthesis of polymer membranes incorporated with GO/ZnO

Polymer solutions having different concentrations of GO and ZnO were prepared by keeping the concentrations of base polymers constant. CA and CS were taken in 0.05% and 0.02% by weight respectively. A measured weight of DMF was used as solvent in the reaction mixture. These polymeric solutions having CS and DMF were subjected to the ultrasonic bath setting vibrations (40 kHz) for 3



Scheme I. Proposed interactions among ingredients of prepared RO membranes.

h at 70 °C to dissolve the materials entirely. Then CA was incorporated in the solution and was stirred for 2–3 h at 70 °C. The solutions were cooled at room temperature and then different concentrations of GO/ZnO were added to each polymeric solution and the solutions once again stirred for 2 h at 60 °C. To get homogenized polymeric solutions, after stirring, the solutions were subjected to ultrasonic bath for 1 h at 60–70 °C. The polymeric solutions having various amounts of GO/ZnO were labeled as GO1 to GO6 and then spread in clean petri dishes with the help of a doctor blade to get fine membranes in terms of uniform thickness. The polymeric GO/ZnO membranes were kept in an oven at 60 °C for drying. After 12 h, the membranes were removed from the vacuum oven and detached from the Petri dish. The thickness of membrane was measured as 24–28 μm using a screw gauge. The proposed physical and chemical interactions among all the ingredients are represented in [Scheme I](#).

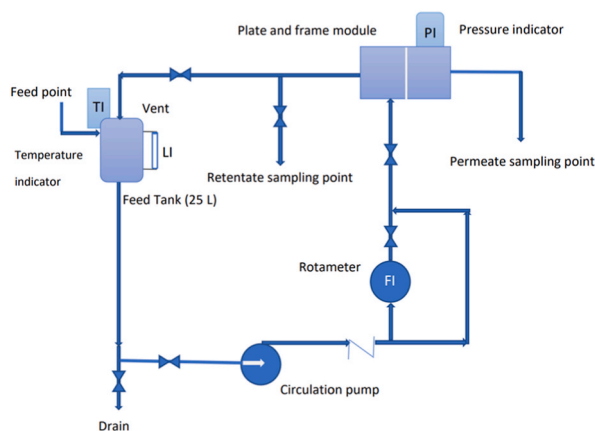


Fig. 1. Flow sheet diagram of reverse osmosis plant in which TI (temperature indicator), LI (level indicator), PI (pressure indicator), FI (flow indicator).

3. Characterizations

3.1. Fourier transform infrared spectroscopy

The synthesized polymeric GO/ZnO membranes were characterized by FTIR. The spectra of membranes were recorded using Cary 630 FTIR instrument (Agilent technologies USA), over the range of 4000–650 cm^{-1} .

3.2. Scanning electron microscopy

Scanning electron micrographs of polymeric membranes were obtained using JEOL (JSM-6480 L V, Japan) scanning electron microscope. The membranes were examined for the surface morphology as well as the core structure of prepared membranes. The GO/ZnO membranes were analyzed on a carbon dioxide conductive tape. The low suction method was used to run membranes tubes at 20 kV.

3.3. Thermal behavior

Polymeric membranes were subjected to thermal properties using a thermogravimetric analyzer [TA instruments SDT Q. 600 V²⁰ 0.9 Build 20 simultaneous differential scanning calorimetry (DSC)/thermogravimetric analysis (TGA)], by heating them from room temperature to 600 °C at a heating rate of 10 °C/min under nitrogen flow.

3.4. Reverse osmosis performance test

RO performance tests were done using a plate and framework membrane module. Humic acid (100 ppm) solution was used as a feed solution of known conductance. The operative area of membrane touching the continuous feed flow was 154 cm^2 . Flux was collected for 12 h in a continual RO procedure. The supplied feed container capability was 25 L as well as feed inlet alongside circulation pump of 1 KW complied with rotameter. RO functionality tests of the GO membranes were studied based upon NOM turn-down, R (%) and permeation flux ($\text{L}/\text{m}^2 \cdot \text{h}$) using Equations (1) and (2). Permeate and retentate were collected during the process coming from their respective sampling aspects. The pressure range during the operation was varied from 200 to 800 Psi. The conductance of the feed and flux was found by using Cyber Scan Waterproof Personal Computer 300 Series (EUTECH). The whole process is displayed in Fig. 1.

$$\text{NOM rejection} = \left[1 - \left(\frac{\text{Permeate conductance}}{\text{Feed conductance}} \right) \right] \times 100 \quad (1)$$

$$\text{Permeate flux} = \frac{\text{Permeate unit (ml)}}{\text{Membrane area (in}^2\text{)} \times \text{time (min)}} \quad (2)$$

3.5. Contact angle

Polymer membranes were analyzed to measure contact angle using SEO Phoenix 300 contact angle analyzer. For this purpose, water was used as the solvent and the volume of sessile drop was kept at 5 μL in all cases by means of a micro syringe. The contact angle dimensions were noted as snap shots per fixed time intervals for a single water droplet.

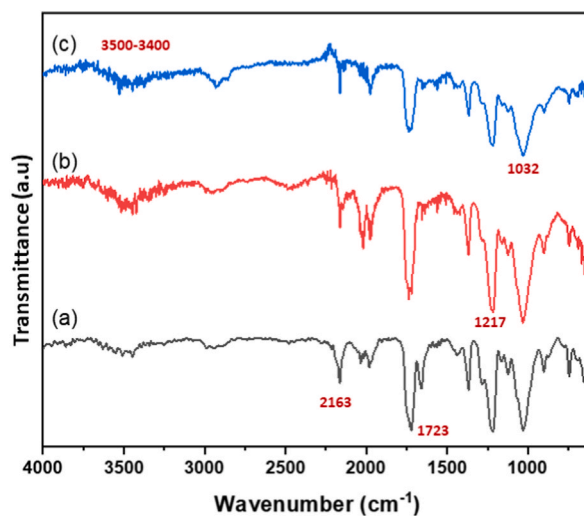


Fig. 2. FTIR spectrum of (a) GO1, (b) GO4, (c) GO6 membrane.

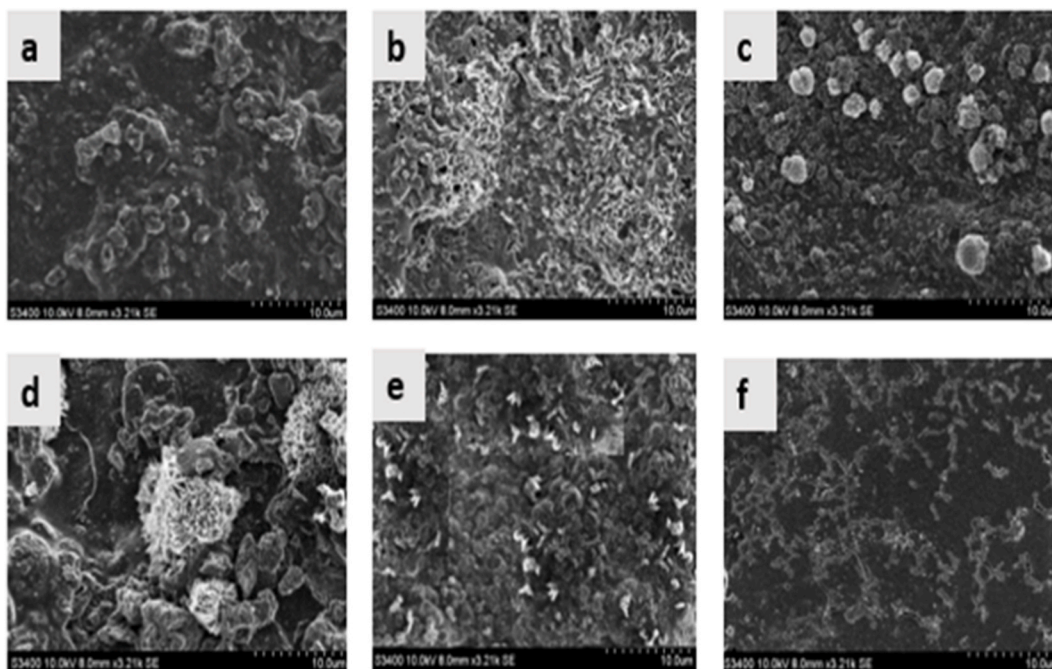


Fig. 3. SEM micrographs for the surface morphology of GO/ZnO membranes (a, b, c, d, e and f representing SEM images of the membranes GO1, GO2, GO3, GO4, GO5 and GO6 respectively).

3.6. Water content

Prepared membranes were dried in an oven at 70 °C under vacuum for 48 h to make them ready for water content analysis. The dried membranes were then kept in a vial of distilled water at room temperature (1 g membrane/100 mL water). The water content of polymeric membranes was calculated after 24 h using Equation (3).

$$WC (\%) = \frac{W_s - D_s}{W_s} \times 100 \quad (3)$$

Where,

WC stands for water content, W_s represents the weight of the wet sample and D_s means the weight of the dry sample.

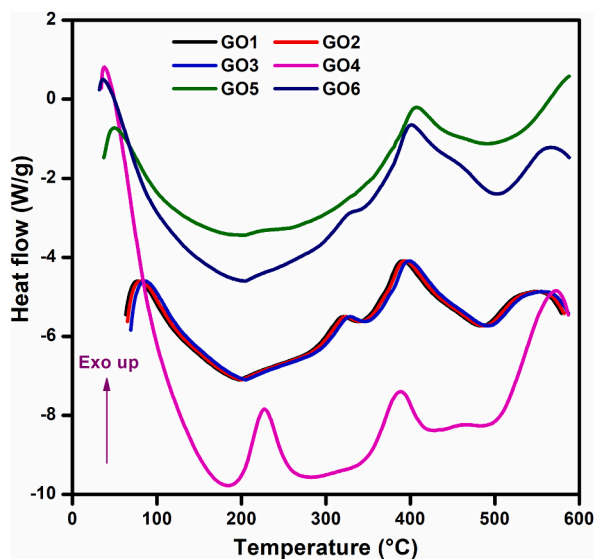


Fig. 4. DSC curves of GO/ZnO membranes.

4. Results and discussion

4.1. Fourier transform infrared spectroscopy

The FTIR spectra of the selected samples GO1, GO4 and GO6 are shown in Fig. 2 (a, b, and c). The spectrum of the membrane GO1 having maximum concentration of ZnO is shown in Fig. 2a. The characteristic broad peak in the region of $3500\text{--}3400\text{ cm}^{-1}$ reveals the existence of hydrogen bonded --OH stretching. A broad band displays the presence of unsaturation near 3000 cm^{-1} in the polymer structure of synthesized membrane. The peculiar sharp peak is evidently observable in the region of triple bond i.e. 2163 cm^{-1} . This peak is shadowed by further additional peaks at 1367 , 1217 and 1032 cm^{-1} , which strongly indicate the presence of a triple bond either $\text{C}\equiv\text{C}$ or $\text{C}\equiv\text{N}$ in the membrane structure. Another sharp peak at 1656 cm^{-1} discloses the presence of simple carbonyl groups. The characteristic peak at 1656 cm^{-1} demonstrates the unsaturation because of $\text{C}=\text{C}$ or $\text{C}\equiv\text{C}$ bond. This spectrum also illustrates the presence of $\text{C}\text{--H}$ bending vibration in the form of certain peaks in the region of $800\text{--}670\text{ cm}^{-1}$ [31].

The peculiar broad band in GO4 membrane in the region of hydrogen bonding indication ($3500\text{--}3400\text{ cm}^{-1}$) recurred in the FTIR spectrum in Fig. 2b, may be illustrating that the balance of ZnO/GO has come within reach of its optimum value. The peak near 2900 cm^{-1} is observed again. Though, the other peaks got sharpened and intensified revealing the effect of change of balance in concentrations of carbonyl $\text{C}=\text{O}$ and $\text{C}\text{--H}$. Perhaps, the increasing concentrations of GO in the GO4 membrane composition is provided that enough space to get the functional groups arranged appropriately, therefore improving the activity of all the bonds [32].

Higher concentrations of GO in GO6 (Fig. 3c) membrane show that all peaks are sharper and more intense than the previous ones. The broader band near 3400 cm^{-1} displays the strong hydrogen bonding by indicating --OH bond stretching. The characteristic sharp peaks at 2927 and 2880 cm^{-1} indicate the presence of asymmetric and symmetric bond stretching of methyl group --CH_3 in the membrane. The sharp peaks at 2165 and 2035 cm^{-1} demonstrate the absorption by $\text{C}\equiv\text{C}$ or $\text{C}\equiv\text{N}$ bond. A very strong and sharp peak at 1723 cm^{-1} represents the occurrence of highly active carbonyl group specifically participating in hydrogen bonding as it is reinforced by a broad peak near 3400 cm^{-1} indicating --OH bond stretching. The peaks at 1367 , 1217 , 1125 , 1032 and 900 cm^{-1} are symbolic of $\text{C}\text{--H}$ stretching [33].

4.1.1. Scanning electron microscopy (SEM)

The surface morphology of the synthesized GO/ZnO membranes was evaluated by SEM images as shown in Fig. 3 (a, b, c, d, e and f). All the Figures clearly represent the dispersion of ZnO particles on GO sheets. The diversity and variation in the surface structure can be observed as the concentration of GO and ZnO changes in the membranes. The membranes were found smooth and dense especially for GO1 and GO6 where ZnO and GO were the only controlling factors respectively. As the concentration of GO and ZnO changed inversely from the membrane GO1 to membrane GO6, the versatility appeared in images reflects a reasonable compatibility among ingredients. The roughness of surface is enhanced as more diverse pores, channels and tubular extensions appear in the polymer structure owing to the incorporation of variety of materials [34]. In the sample GO4, where a comparable amounts of GO and ZnO has been embedded, intense ups and downs can be identified. The morphological structure seems to be changed from having finger-like projections to macro-voids. This may be explained by taking in consideration, the fast liquid-liquid demining of GO membranes in water which makes the membranes more compatible with water. Such morphological structure may be helpful while absorbing aqueous medium [35].

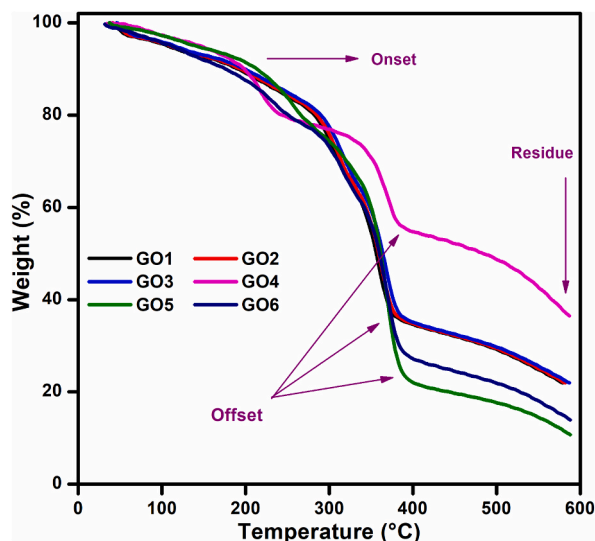


Fig. 5. TGA thermograms of GO/ZnO membranes.

4.2. Differential scanning calorimetry (DSC)

DSC is a very valuable tool and used often to study the thermal behavior of various blended polymers. This analysis gives information about glass transition temperature (T_g), melting temperature (T_m) and crystallization temperature (T_c) of all kinds of polymers [36]. Fig. 4 shows the DSC thermograms of CA/CS polymeric membranes blended with GO and ZnO content added in reverse order of concentration with respect to each other. No GO amount has been incorporated to GO1 membrane whereas the maximum amount of ZnO is added which controls the thermal stability principally. On the other hand, in GO6 membrane bearing maximum amount of GO with zero content of ZnO. Mutual outcome of comparable ratio of GO/ZnO on DSC curves of CA and CS blended membranes can be detected in membranes. It is evidently shown that T_g for the membranes under observation, is nearly 200 °C which is highly elevated as compared to the T_g (~55 °C) of CA in its pure form. This shift of T_g to a higher temperature designates the enhanced thermal permanency caused due to development of robust interactions either due to hydrogen bonding development among functional groups of CA and CS or appearance of covalent cross-links due to chemical bond establishment between polymer chains or even the ion-dipole interactions appeared due to the addition of ZnO. Greater value of T_g also approves less free volume resulting limited movement of chains is practiced by these fabricated membranes. It has been described that plain CA/CS polymer membranes without extra additive show T_g value of 200–350 °C [37].

Furthermore, the endothermic heat flow of GO4 membrane with equal ratio of GO/ZnO is maximum as compared to other GO membranes. It is attributed to the strong interactions produced because of the combined synergetic effect of GO and ZnO, that likewise generates a rational packing density inside the various membranes. Nevertheless, the heat flow is decreased in the samples GO5 and GO6, may be because of lesser concentration of ZnO which in turn lacks stronger ion-dipole interactions. Broader endothermic peak is unveiled in all the membranes close to 400 °C which portrays the additional stability for applied temperature. Hence, it can be claimed that the joint endeavor of GO and ZnO has produced improved chain stiffness, amplified crosslink density, inadequate chain mobility and ultimately anomalous enhanced thermal stability to these blended membranes. The shifting of T_g towards higher temperature also specifies the thermal stability of CA/CS blend membranes, perhaps due to restricted segmental movements [38].

4.3. Thermogravimetric analysis (TGA)

The thermal behavior of CA/CS membranes incorporated with GO and ZnO was found important enough to gain valuable information about their peculiar thermal parameters. The TGA curves of these membranes in which the amounts of GO and ZnO are diversified has been shown in Fig. 5. The thermograms display an emblematic three step decomposition of CA based membrane. Customarily, it gives the impression that addition of variety of components into the CA network changes its thermal stability in diverse manner. First step shows the definite volatilization and dehydration of entrapped water starting from ~30 °C and ending at ~250 °C [39]. Various amounts of GO and ZnO appear to have no rational effect on first step approach of synthesized membranes. The second step indicates the variation in thermal performance due to the occurrence of different components with various amounts. The membranes having different concentrations of GO and ZnO (either GO>ZnO or ZnO>GO) do not show a protruding deviation in behavior. Conversely, sample GO4 (having GO \cong ZnO) is revealing an extra ordinary thermal stability and two-step process of thermal degradation. In thermograms, a tiny initial loss of mass is detected in the temperature range of 260–320 °C and can be consigned to the loss of water present in the GO. The second degradation step shown in the temperature range of 320–400 °C is ascribed to pyrolysis of the changing oxygen bearing functional groups forming CO, CO₂ and water vapors [40]. CO₂ formation by decarboxylation turns into

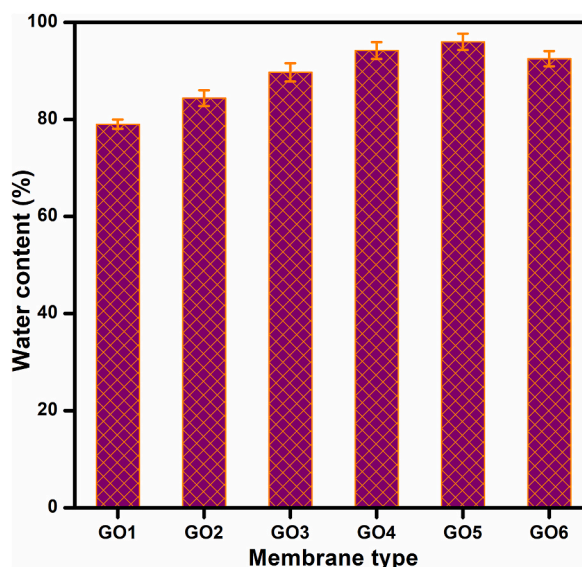


Fig. 6. Water Content (%) of GO/ZnO membranes versus composition of membranes (wt%).

more and more significant above 250 °C and unceasing emission of both water and CO₂ takes place up to 400 °C. The increased amounts of GO prolong the degradation phenomenon in the membranes [41] whereas a direct relationship between GO content and thermal stability was detected in GO/PAA-g-amylose nanocomponents [42].

In GO4, both GO and ZnO are existing almost in equal amounts, so they produce reduction in the mobility of polymer chain by their strong interactions. As the chain mobility is restricted, it provides chain transfer reaction to be suppressed, ensuing in slower degradation process and happening of decomposition at higher temperature. The thermal behavior exhibited is considered to be the consequence of strong interfacial interaction between GO and ZnO along with CA and CS polymer material. GO is also responsible to perform as a mass generated as volatile products during the process of degradation, thus augmenting the thermal stability of designed membranes. GO and ZnO both are subsidizing to decide the degradation performance of polymeric membrane. This can be attributed to intense interaction between ZnO and oxygen atoms of the CA structure [43].

4.4. Water content

The ability of membranes to carry water is a matter of their hydrophilic nature [44]. The amount of water accommodated by GO membranes is presented in terms of percentage water content (%) in Fig. 6. It was found that the concentration of GO and ZnO in the polymer matrix affects the water content constructively. The membrane GO1 was dealt as control with respect to GO as it was prepared with zero amount of GO and maximum content of ZnO. A sequential improvement in water content was observed from GO1 to GO5 (water content was 76–96%) whereas the membrane GO6 has a decline in water content that was reduced to 92.5%. There was no synergistic effect of GO and ZnO in membranes GO1 (GO:ZnO: 0.0:0.18) and GO6 (GO:ZnO: 0.18:0.00). It may be analyzed as the concentration of ZnO is decreased, more water is available to be accommodated in the porous structure of GO; other than most of the water was used to hydrate ZnO ions. As the content of GO was increased, more surface was available to absorb water. However, the ZnO content was helping to break hydrogen bonds in aqueous medium, thus facilitating the availability of water to get accommodated inside the membrane. Whereas in GO6, there was a little bit decrease in water content from 96 to 92.5%. In fact, the optimum interaction between GO and ZnO to control the hydrophilicity of membranes was exhibited in GO5. Moreover, the decrease in concentration of ZnO from GO1 to GO5 may reduce interionic crosslinks in the polymer matrix, again supporting the hydrophilic nature of membranes [45].

4.5. Transport properties of membranes: permeate flux

The transport properties of GO based membranes were analyzed, studying the permeate flux of a 100 ppm humic acid solution and the deionized water to compare the effect of amount of NOM in the model solution on the efficiency of membranes. All the considerations were restricted to the optimized conditions of pressure and temperature (800 psi and 25 °C). The measured flux values are plotted against GO:ZnO concentrations as shown in Fig. 7. It is clear that the constructive interaction of increased amounts of GO and decreased quantity of ZnO is persistent as was studied in the case of water content. The maximum flux was exhibited by GO5 (360 L/m²h for DI and 324 L/m²h for humic acid), owing to its optimum hydrophilicity, that was two times higher than that exhibited by GO6. The enhanced permeate flux is the result of variety of porosity experienced by GO membranes. The pore diversity plays a vital role in tuning the transport characteristics of membranes [33].

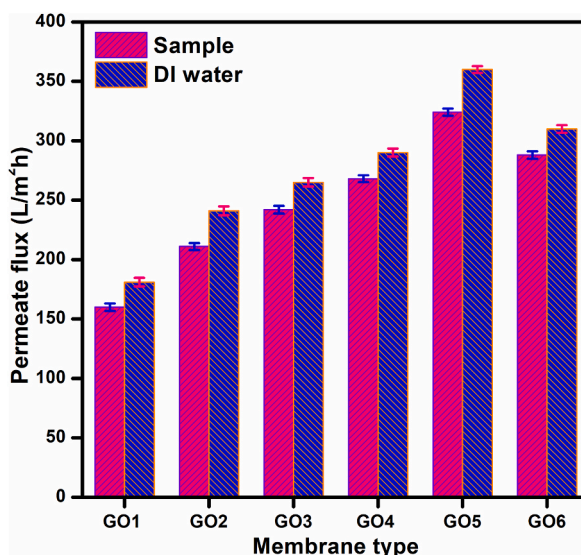


Fig. 7. Comparison of the permeation fluxes (L/m^2h) with different feed solutions (pressure 800 psi).

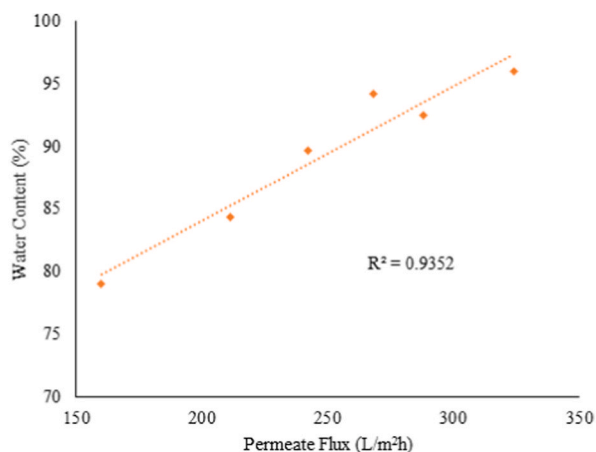


Fig. 8. Relationship between water content and permeate flux.

A similar trend is noticed for humic acid solution and DI water. However, all the membranes performed better in case of DI water than that for the sample solution. In humic acid solution, the organic content is reluctant to be adsorbed in membranes whereas DI water feels free while getting affiliated with membranes.

Moreover, a good correlation factor is observed while plotting the water content against permeate flux as is given in Fig. 8. It is suggested that these membranes exhibit a parallel behavior between the two factors.

4.6. Contact angle

The membranes were studied regarding contact angle and the results are shown in Fig. 9. The comparatively smooth membranes of GO1, as discussed in SEM micrographs, presented a contact angle of 63° , showing a comparatively hydrophobic character of GO membranes. However, introduction of graphene oxide in GO2 and onwards, reduced the angle almost in a regular way. Lesser is angle, more hydrophilic is the membrane [45]. As the amount of GO increased and that of ZnO decreased, a great diversity was introduced in the morphology of membranes, which results in decline in contact angle from 63° to 36° . The reduction in contact angle is the prediction for improved hydrophilicity and enhanced wetting capacity of the membrane topography, so it is proposed that GO is responsible to introduce higher roughness to the surface, thus affecting contact angle adversely. The morphological and top de-neatness trend exhibited by these specific systems are in correspondence with other researches in the literature [46].

The minimum contact angle was observed in GO5. In membrane GO6, an increase in the angle was observed from 36° to 49° . As in GO6, there was no ZnO amount so the roughness was gradually modified into smoothness of the surface thus reducing absorption

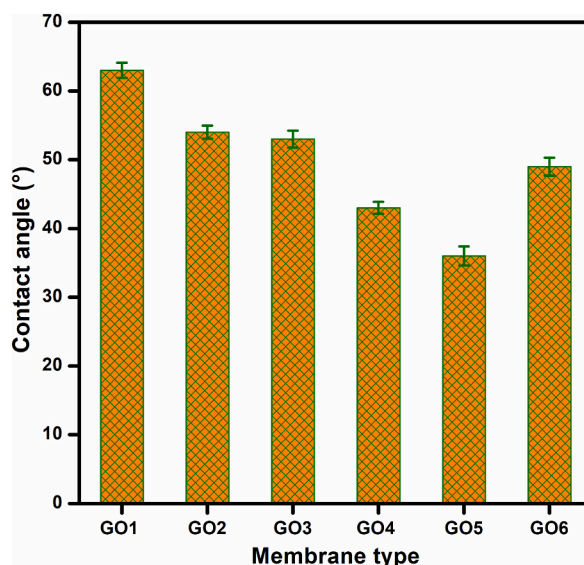


Fig. 9. Effect of Concentration of MWCNTs on Contact angle.

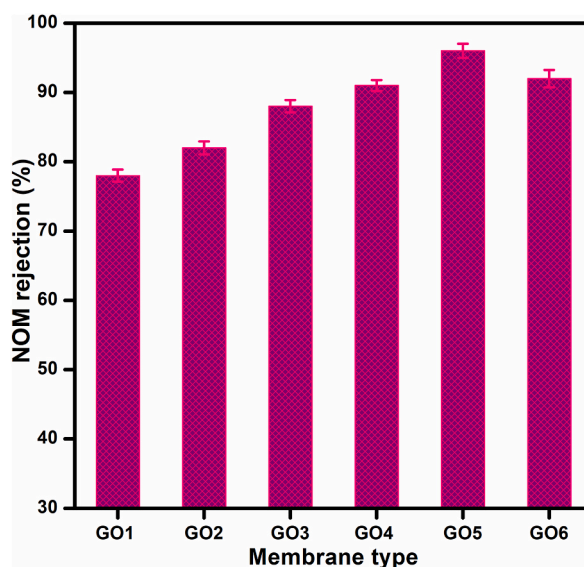


Fig. 10. NOM rejection (%) of various GO/ZnO modified membranes.

capacity of the membrane. In membranes from GO1 (with highest amount of ZnO) to GO5 (minimum quantity of ZnO), the contact angle was found to be directly related to the ZnO concentration in the membranes (63° – 36°), so the melting capacity of the membranes has been converted from hydrophobic to the hydrophilic when ZnO impregnation is reduced from GO1 to GO5 [47]. The hydrophobic characteristics of membranes having ZnO incorporated in them, are highly prominent which may be attributed to the presence of interspaces among ZnO particles, facilitating the air trapped in them. As the contact angle of air is considered 180° ; so general surface of the membrane resulting in the formation of solid/air blended surface to enhance the hydrophobicity of the membrane [48]. Similar effect of ZnO has been reported in literature when ZnO content was increased in cellulose/ZnO, an increase in contact angle and improvement in hydrophobic character was observed in them⁴². On the other hand, addition of SGO (Sulphonated Graphene Oxide) in CA/SGO composite membrane improved hydrophilic character and exhibited in the form of regular decrease in contact angle [49]. In these GO/ZnO membranes, the concentration of GO was increased with the decrease in ZnO so both synergized the hydrophilic ability of these membranes.

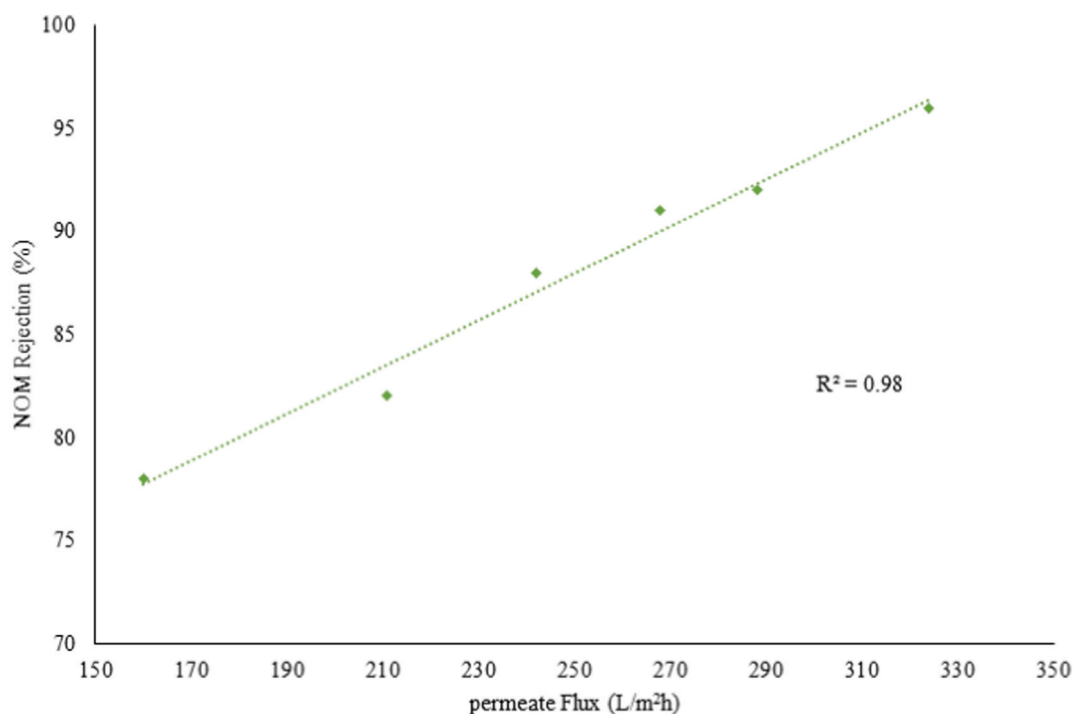


Fig. 11. Linear relationship between NOM rejection and permeate water flux.

Table 1

Descriptive statistics of prepared membranes.

	Minimum	Maximum	Mean	Std. Deviation	Skewness	Std. Error
Flux (L/m ² .h)	160.00	324.00	248.8333	58.17359	-0.402	0.845
NOM Rejection (%)	78.00	96.00	87.8333	6.70572	-0.498	0.845

4.7. NOM rejection

The quantitative analysis of novel synthesized membranes for NOM rejection is usually carried out by studying their absorption capacity in UV range at the optimum wavelength of 254 nm (UV-254). The feed solution prepared for this purpose in this specific case was 100 ppm humic acid (HA). The percentage NOM rejections with respect to the varying concentration of GO/ZnO is plotted in the graph as shown in Fig. 10. A reasonable efficiency for removal of the NOM was displayed by the membranes. A prominent increase in NOM rejection takes place when the concentration of GO changes from 0.00% to 0.018 wt % and that of ZnO from 0.018 wt % to 0.00 wt %. Both GO and ZnO synergized the NOM rejection efficiency from 79% to 96%. A good interdependency can be noticed between GO and NOM rejection capacity of membranes. Low NOM rejection (73% only) by GO1 membrane is because of comparatively neat surface as already discussed in SEM analysis. Similar link between neatness of the membrane surface and the protein rejection is reported in literature [25]. In membranes GO2 to GO5, both GO and ZnO inversely added in the host polymer matrix co-facilitate the NOM rejection. On the other hand, the comparison of NOM rejection by GO1 (GO:ZnO:0.00:0.18) and GO6 (GO:ZnO: 0.18:0.00) indicates that the incorporation of GO in the membrane proves to be a better controlling factor than ZnO, not only in case of NOM rejection but also for water permeate flux and water content capturing capability. Results shows the 92% NOM rejection by GO6 which is 14% greater than that displayed by GO1 which rejects only 78% NOM.

Furthermore, these GO membranes seem to hit the most remarkable balance between NOM rejection and permeate flux as shown in Fig. 11.

4.8. Statistical analysis

The statistical analysis was adopted for evaluating the performance of synthesized GO/ZnO blended membranes. The average flux for this series of membrane was 28.333 (L/m².h) with standard deviation of 58.1736 having a very slight negative skewness. On the other hand, for 6 observations of NOM, the average rejection percentage was observed to be 87.8333 which was noticeably high with comparatively lower value of standard deviation of 6.7057 (Table 1).

These membranes produced a very high correlation coefficient which was approximately equal to 1, i.e. the correlation coefficient

Table 2
ANOVA analysis of prepared membranes.

Model	Sum of Squares	Df	Mean Square	F	Sig.
Regression	220.327	1	220.327	195.573	0.000
Residual	4.506	4	1.127		
Total	224.833	5			

value was $r = 0.99$ showing that there was a perfect positive correlation between flux and NOM with very positive slope. Taking into consideration the values of R^2 and adjusted R^2 were found to be 0.98 and 0.975 respectively, this showed that the variation was about 97.5% completely explained.

For regression model and its analysis using ANOVA, the following results were obtained showing the regression Equation (4):

$$\text{NOM} = 59.439 + 0.114 \text{ Flux} \quad (4)$$

In the above model, the regression equation coefficients were found to be highly significant i.e. the p-value was 0.000 at even 1% level of significance.

In the given Table 2 of ANOVA, it was observed that the model estimated above was highly significant with a F-value = 195.573, which was highly significant at 1% level of significance. Hence, this analysis gave the evidence that the synthesized membranes have the greater permeation along with the highest NOM rejection which is in turn helpful to remove pollutants and increase the quantity of reusable water.

5. Conclusions

CA/CS membranes loaded with GO and ZnO have been fabricated successfully by solution casting method. The DSC and TGA results reveal that the synthesized GO based membranes acquire a reasonable thermal stability. All the FTIR graphs demonstrated that GO nano-sheets were compatible with CA and CS polymer matrix owing to the strong hydrogen bonding introduced between carbonyl group of CA, $-\text{NH}_2$ group of CS and carboxylic groups of GO, ultimately revealing the successful fabrication of new membranes. SEM micrographs displayed the appearance of strongly exfoliated structure and the uniform dispersion of GO content in the polymer matrix. The regular transformation of permeation flux, contact angle, NOM rejection and water content with synergistic control of GO and ZnO content inversely related to each other indicate the fact that the newly synthesized membranes can be tuned by changing the composition of membranes. Consequently, it is deduced that the CA/CS membranes loaded with specific amounts of GO and ZnO have been formed and are proving themselves an optimistic source to be used for water treatment successfully.

Author contribution statement

Rizwana Shami: Performed the experiments; Analyzed and interpreted the data; Wrote the paper.

Aneela Sabir: Conceived and designed the experiments.

Sadia Sagar Iqbal, Shahzad Maqsood Khan: Contributed reagents, materials, analysis tools or data.

Nafisa Gull: Analyzed and interpreted the data; Contributed reagents, materials, analysis tools or data.

Rubab Zahra: Analyzed and interpreted the data.

Funding statement

This research did not receive any specific grant from funding agencies in the public, commercial, or not-for-profit sectors.

Data availability statement

Data will be made available on request.

Declaration of interest's statement

The authors declare that they have no known competing financial interests or personal relationships that could have appeared to influence the work reported in this paper.

References

- [1] I. Ali, M.A. Raza, R. Mehmood, A. Islam, A. Sabir, N. Gull, B. Haider, S.H. Park, R.U. Khan, Novel maleic acid, crosslinked nanofibrous chitosan/poly (vinylpyrrolidone) membranes for reverse osmosis desalination, *Int. J. Mol. Sci.* 21 (2020) 7338–7351.
- [2] E.O. Ezugbe, S. Rathilal, Membrane technologies in wastewater treatment: a review, *Membranes* 10 (2020) 89.
- [3] C.J. Vorosmarty, P. Green, J. Salisbury, B. Richard, R.B. Lammers, Global water resources: vulnerability from climate change and, *Population Growth* 289 (2000) 284–288.
- [4] H.C.J. Godfrey, J.R. Beddington, I.R. Crute, Food Security: the challenge of feeding 9 billion people, *Science* 327 (2010) 812–818.

- [5] K. Mulder, N. Hagens, B. Fisher, Burning water: a comparative analysis of the energy returns on water invested, *Ambio* 39 (2010) 30–39.
- [6] J.C. Bowman, J.L. Zhou, J.W. Readman, Sediment- Water interactions of natural estrogens under estuarine conditions, *Mar. Chem.* 77 (2002) 263–276.
- [7] M. Verstraeten, T. Heberer, J.R. Vogel, T. Speth, S. Zuelhke, U. Duennbier, Occurrence of endocrine-disrupting and other wastewater compounds during water treatment with case studies from Lincoln, Nebraska and Berlin, Germany, *Pract. Period. Hazard. Toxic, Radioact. Waste Manag.* 7 (2003) 253–263.
- [8] H. Ozaki, Rejection of micropollutants by membrane filtration, in: *In Proceedings of the Regional Symposium on Membrane Science and Technology, Johor, Malaysia, 2004.*
- [9] M.R. Servos, D.T. Bennie, B.K. Burnison, Distribution of estrogens, 17 β -estradiol and estrone, in Canadian municipal wastewater treatment plants, *Sci. Total Environ.* 336 (2005) 155–170.
- [10] T. Urase, T. Kikuta, Separate estimation of adsorption and degradation of pharmaceutical substances and estrogens in the activated sludge process, *Water Res.* 39 (2005) 1289–1300.
- [11] M. Petrovic, A. Diaz, F. Ventura, Barcelo, Occurrence and removal of estrogenic short chain ethoxy nonylphenolic compounds and their halogenated derivatives during drinking water production, *Environ. Sci. Technol.* 37 (2003) 4442–4448.
- [12] P. Westerhoff, Y. Yoon, S. Synder, E. Wert, Fate of endocrine disruptor, pharmaceutical and personal care product chemicals during simulated drinking water treatment process, *Environ. Sci. Technol.* 39 (2005) 6649–6663.
- [13] N. Vieno, T. Tuhkanen, L. Kronberg, Removal of pharmaceuticals in drinking water treatment. Effect of chemical coagulation, *Environ. Technol.* 27 (2006) 183–192.
- [14] W. Zhang, F.A. DiGiano, Comparison of bacterial regrowth in distribution systems using free chlorine and chloramine: a statistical study of causative factors, *Water Res.* 36 (2002) 1469–1482.
- [15] R. Gopal, K. Satinderpal, Y.F. Chao, C. Casey, R. Seeram, T. Shahram, M. Takeshi, Electrospun nanofibrous polysulfone membranes as pre-filters: particulate removal, *J. Membr. Sci.* 289 (2007) 210–219.
- [16] E.M. Thurman, *Organic Geochemistry of Natural Waters*, Martinus Nijhoff/Dr W. Junk Publishers, Boston, Mass, USA, 1985.
- [17] G.R. Aiken, D.M. McKnight, K.A. Thorn, E.M. Thurman, Isolation of hydrophilic organic acids from water using nonionic nonporous resins, *Org. Geochem.* (1992) 567–573.
- [18] A.W. Zularisam, A.F. Ismail, R. Salim, Behaviors of natural organic matter in membrane filtration for surface water treatment- a review, *Desalination* 194 (1–3) (2006) 211–231.
- [19] V. Uyak, M. Akdagli, M. Cakmacki, I. Koyuncu, Natural Organic Matter removal and fouling in low pressure hybrid membrane, *Sci. World J.* 2014 (2014) 1–2.
- [20] M. Yao, L.D. Tijing, G. Naidu, S.H. Kim, H. Matsuyama, A.G. Fane, H.K. Shone, A review of membrane wettability for the treatment of saline water deploying membrane distillation, *Desalination* 479 (2020), 114312.
- [21] Y. Yu, Y. Yang, K.Y. Koh, J.P. Chen, Modification of polyvinylidene fluoride membrane by silver nanoparticles-graphene oxide hybrid nanosheet for effective membrane biofouling mitigation, *Chemosphere* (2020), 129187.
- [22] R. Haddad, E. Ferjani, M.S. Roudelsi, A. Deratani, Properties of cellulose acetate nanofiltration membranes. Application to brackish water desalination, *Desalination* 167 (2004) 403–409.
- [23] O. Kuttoway, S. Sourirajan, Cellulose acetate ultrafiltration membranes, *J. Appl. Polym. Sci.* 19 (1975) 1449–1460.
- [24] M. Sivakumar, R. Malaisamy, C.J. Sajitha, D. Mohan, V. Mohan, R. Rangarajan, Ultrafiltration application of CA-PU blend membranes, *Eur. Polym. J.* 35 (1999) 1647–1651.
- [25] C.L. Lv, Y.L. Su, Y.Q. Wang, X.L. Ma, Q. Sun, Z.Y. Jiang, Enhanced permeation performance of cellulose acetate ultrafiltration membrane by incorporation of Pluronic F127, *J. Membr. Sci.* 294 (2007) 68–74.
- [26] A. Alkhouzaam, H. Qiblawey, Novel polysulfone ultrafiltration membranes incorporating polydopamine functionalized graphene oxide with enhanced flux and fouling resistance, *J. Membr. Sci.* 620 (2021) 118900–118903.
- [27] Y. Zhang, T.-S. Chung, Graphene oxide membrane for nanofiltration, *Curr. Opin. Chem. Eng.* 16 (2017) 9–15.
- [28] N. Song, X. Gao, Z. Ma, X. Wang, Y. Wel, C. Gao, A review of graphene-based separation membrane materials, characteristics, preparation and applications, *Desalination* 437 (2018) 59–72.
- [29] K. Malachová, P. Praus, Z. Rybková, O. Kozak, Antibacterial and antifungal activities of silver, copper and zinc Montmorillonites, *Appl. Clay Sci.* 53 (2011) 642–645.
- [30] E. Zanni, C. Chandraihaigari, G. De Bellis, M. Montereali, G. Armiento, R.P. Ballirano, A. Polimeni, M. Sarto, D. Uccelletti, Zinc oxide nanorods-decorated graphene nanoplatelets: a promising antimicrobial agent against the carcinogenic bacterium *Streptococcus mutans*, *Nanomaterials* 6 (2016) 179.
- [31] W. Chong, E. Mahmoudi, Y. Chung, M. Ba-Abbad, C. Koo, A. Mohammad, Polyvinylidene fluoride membranes with enhanced antibacterial and low fouling properties by incorporating ZnO/rGO composites, *Desalination Water Treat.* 96 (2017) 12–21.
- [32] O.T. Mahlangu, R. Nackaerts, J.M. Thwla, B.B. Mamba, A.R.D. Verliefde, Hydrophilic fouling-resistance GO-ZnO/PES membranes for wastewater reclamation, *J. Membr. Sci.* 524 (2017) 43–55.
- [33] D. Xu, S. Hein, K. Wang, Chitosan membrane in separation applications, *Mater. Sci. Technol.* 24 (2008) 1076–1087.
- [34] S.S. Madaeni, A.H. Taheri, Effect of casting solution on morphology and performance of PVDF microfiltration membranes, *Chem. Eng. Technol.* 34 (2011) 1328–1334.
- [35] S.A. Hosseini, S. Babaei, Graphene oxide/Zinc oxide (GO/ZnO) nanocomposite as a superior photocatalyst for degradation of Methylene Blue (MB)- process modeling by response surface methodology (RSM), *J. Braz. Chem. Soc.* 299–307 (2017) 28.
- [36] W.G. Osiris, T.H.M. Manal, Thermal and structural studies of poly(vinyl alcohol) and hydroxyl propyl cellulose blends, *Nat. Sci.* 4 (2012) 57–67.
- [37] A. Muddasir, M. Zafar, T. Jamil, M.T.Z. Butt, Influence of glycol additives on the structure and performance of cellulose acetate/zinc oxide blend membranes, *Desalination* 270 (2011) 98–104.
- [38] A. Alkhouzaam, H. Qiblawey, Functional GO-based membranes for water treatment and desalination: fabrication methods, performance and advantages. A review, *Chemosphere* 274 (2021), 129853.
- [39] X. Wu, L. Wang, C. Wu, J. Yu, L. Yie, G. Wang, P. Jiang, Influence of char residues on flammability of EVA/EG, EVA/NG and EVA/GO composites, *Polym. Degrad. Stab.* 97 (2012) 54–63.
- [40] J.L. Feunte, M. Wilhem, H.W. Spiess, E.L. Madruga, M.F. Garcia, M.L. Cerrada, Thermal, morphological and rheological characterization of poly(acrylic acid-g-styrene) amphiphilic graft copolymer, *Polymer* 46 (2005) 4544–4553.
- [41] A. Zahra, R.M. Aghdam, M.S. Niasari, S. Shakhesi, Enhanced thermal resistance of GO/C/phenolic nanocomposite by introducing ZnBr₂ nanoparticles, *Compos Part B* 76 (2015) 174–179.
- [42] S.W. Zhao, C.R. Guo, Y.Z. Hu, Y.R. Guo, Q.J. Pan, The preparation and antibacterial activity of Cellulose/ZnO composite: a Review, *Open Chem* 16 (2018) 9–20.
- [43] Z. Amirssardari, R.M. Aghdam, M.S. Niasari, S. Shakhesi, Enhanced thermal resistance of GO/C phenolic nano composite by introducing ZnBr₂ nanoparticles, *Composites Part B* 76 (2015) 174–179.
- [44] Y. Chen, J. Zhang, J. Liu, H. Zhang, K. Wang, Preparation and antibacterial property of polyethersulfone ultrafiltration hybrid membrane containing halloysite nanotubes loaded with copper ions, *Chem. Eng. J.* 210 (2012) 298–308.
- [45] H.K. Okoro, L. Ndewana, Monisola, I. Ikhile, T.G. Barnard, J.C. Ngila, Hyperbranched polyethyleneimine-modified polyether-sulfone (HPEI/PES) and nAg@HPEI/PES membranes with enhanced ultrafiltration, antibacterial and antifouling properties, *Heliyon* 7 (2021), eo7961.
- [46] J.W. Chen, Y.L. Su, L.L. Zheng, L.J. Wang, Z.Y. Jiang, The improved oil/water separation performance of cellulose acetate-grafted polyacrylonitrile membranes, *J. Membr. Sci.* 337 (2009) 98–105.

- [47] S. Anitha, B. Brabu, D.J. Thiruvadigal, C. Gopalerkrishna, T.S. Natarajan, Optical, bactericidal and water repellent properties of electrospun nano-composite membranes of cellulose acetate and ZnO, *Carbohydr. Polym.* 971 (2013) 856–863.
- [48] F. Fu, Lil, J. Cai, Y. Zhang, J. Zhou, J. Zhang, Construction of cellulose based ZnO nanocomposite films with antibacterial properties through one step coagulation, *ACS Appl. Mater. Interfaces* 71 (2015) 2597–2606.
- [49] M. Zahid, A. Rashid, S. Akram, H.M.F. Shakir, Z.H. Rehan, T. Javed, R. Shabbir, M.M. Hessem, Fabrication and characterization of sulphonated graphene oxide-doped polymeric membranes with improved anti- biofouling behavior, *Membranes* 11 (2021) 563.